J. Phys. D: Appl. Phys. **30** (1997) 2261–2269. Printed in the UK PII: S0022-3727(97)69440-1

REVIEW ARTICLE

The production of active plasma species for surface treatments

A Ricard†

LPGP, Bâtiment 212, Université Paris-Sud, 91405 Orsay Cedex, France

Received 7 October 1996, in final form 1 April 1997

Abstract. Plasma technology is progressing rapidly, although there is still a need for much research and development. *In situ* diagnostics such as emission spectroscopy are set up to control the plasma processes. Two experiments concerning treatments of polymer and steel surfaces using a flowing post-discharge plasma of O_2 and N_2 are described. The diagnostics of O and N atom densities have been correlated to the surface activity (for the polymer) and to the coating formation (for steel). Poisoning of the glass tube walls of the flowing discharge and post-discharge reactors was achieved by introducing a little N_2 into H_2 or a little H_2 into N_2. We observed a detectable increase in density of atoms of the dominant gas species in both cases.

1. Introduction

Plasma technology allows surface treatments at low gas temperatures (300 K for polymers, 600 K for semiconductors, 800–1000 K for metals and diamond-like films), rapid and automatic processes and the fabrication of new artificial coatings with extreme properties, for example ceramics for high-temperature resistances, diamond-like films for hardness and high thermal conductivity (for efficient cooling of electronic structures) and superconductors. Moreover, plasma processes at low gas pressures are more subtle than are traditional chemical processes.

Research and development plays a very active role in plasma technology. In France [1], plasma surface treatments amount to about 2% of the total number of treatments in mechanical industries; however, research and development efforts and needs are an order of magnitude higher. The main plasma treatments in mechanical industries are plasma nitriding (34%), plasma vapour deposition (PVD) (27%) and plasma spraying (36%). Plasma nitriding is applied to increase the resistance to wear and corrosion and to decrease the friction of workpieces, for example in the automotive and nuclear industries.

PVD, which is dominated by TiN coatings, is mainly applied for hard coatings on cutting and extrusion tools. Plasma spraying deposits thick coatings at a high deposition rate, mainly for aeronautical applications (50%).

In this paper, the author reports experimental results concerning non-equilibrium plasmas (hot electrons, cold neutral atoms or molecules) which are the sources for active species in surface treatments. For each application, correlations between the production of active species in the plasma and the chemical transformations of the treated surfaces are disclosed. In particular, the potentiality of flowing discharge reactors is discussed.

2. Plasmas for polymer treatments

Plasma treatments of polypropylene surfaces are performed in order to increase the adhesion properties in order to promote grafting and inking operations. The adhesion properties of polypropylene depend on the surface polar energy which is measured by the drop-angle method. To avoid both too high a neutral gas temperature and a perturbation of treated surfaces by ionized species in the plasma, a flowing post-discharge treatment appears to be the most convenient method [2]. An oxygen post-discharge reactor is shown in figure 1. The set-up is a flowing microwave discharge in oxygen gas at a mean pressure of 1 Torr and approximately 100 W power. The discharge is produced in a side-arm tube to avoid interaction of the plasma's light with the substrate. The effect of UV light on the polymer surface was studied by irradiating the surface using a mercury lamp.

It has been observed [2] that the increase in surface activity is caused by oxygen atoms rather than $O_2(^1\Delta)$ metastable molecules. Indeed, a tungsten mesh was introduced into the post-discharge tube (see figure 1), removing the oxygen atoms and selecting the $O_2(^1\Delta)$ which are not destroyed by reaction with the W mesh [2]. It was then observed that the polypropylene surface was only

† Present address: CPAT, Université Paul Sabatier, 118 Route de Narbonne, 31062 Toulouse Cedex 4, France.

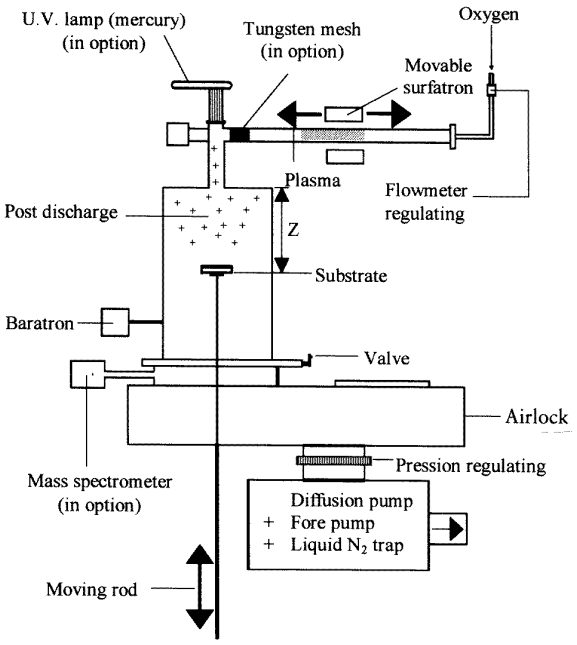

Figure 1. The microwave post-discharge reactor for treatment of polypropylene.

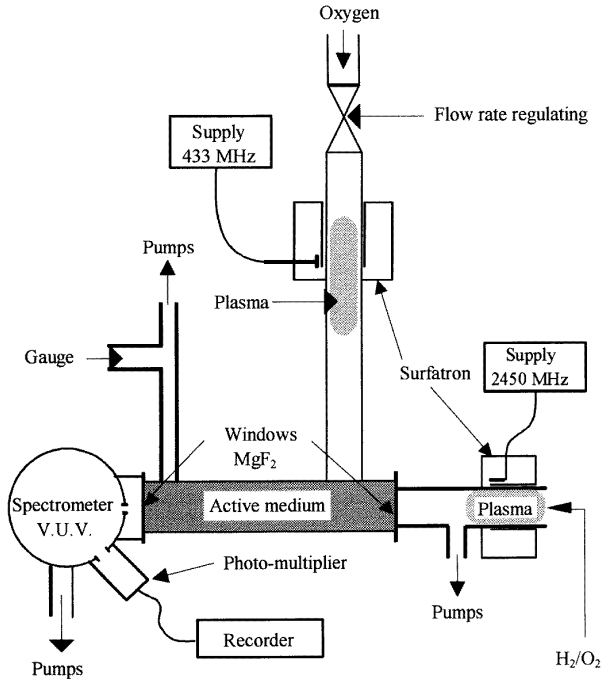

Figure 2. The experimental set-up for measurement of the oxygen atom density by VUV optical absorption in a microwave flowing post-discharge reactor.

slightly modified by the $O_2(^1\Delta)$ molecules. Consequently, it was deduced that the O atoms were the only active species. The oxygen atom density was determined by VUV optical absorption as shown in figure 2 [3].

The VUV optical absorption measurement was performed by means of an O_2 optical source which emitted the O I 130.2 nm spectral line whose profile was recorded with a 10 m focal length VUV spectrometer (located in the Meudon Observatoire near Paris) whose spectral resolution is 5×10^{-3} Å. Note that the self-reversed profiles of the source oxygen lines are included in the calculations which relate the measured absorption coefficient $A_L = 1 - I_t/I_0$ (I_0 and I_t are the emitted and transmitted total line intensities, respectively) to the O atom density [4].

It was concluded that the surface oxygen atom density in the plasma reactor of figure 1 must be higher than 10^{14} atoms cm^{-2} for it to increase the surface activity of polypropylene (for treatment times 15–3800 s). Indeed, the adhesion of polypropylene increased with its polar energy. The variation in polar energy with O_s, the surface oxygen atom density ($O_s = 1/4$ [O] $\bar{v}t$, where [O] is the oxygen atom density, $\bar{v}$ is the thermal velocity, $\bar{v} = 630$ ms^{-1} at 300 K and t is the treatment time) is reproduced in figure 3 [2].

The polar energy at first increased with the oxygen atom density and then attained a saturation value of about 10^{15} atoms cm^{-2}. As the oxygen atom density increased, the following atomic recombination process became effective at limiting the O atom density:

$$O + O + M \rightarrow O_2 + M \qquad (1)$$

where M denotes the polypropylene surface. Reaction (1) brings an energy of 5 eV to the surface, degrading the polar function. This effect can explain the saturation of polar energy observed in figure 3.

3. Plasmas for metal surface nitriding

3.1. The ion nitriding process

The nitriding process is employed to harden the surfaces of metal workpieces. This process has largely been developed with ion nitriding in industrial reactors in which the metal workpiece is the cathode of a N_2–H_2 glow discharge which is produced inside a heating device at temperatures up to 600 °C [5]. Such a temperature is necessary in order to stabilize the nitrided layers, as is shown by the Fe–N phase diagram in figure 4. At $T = 570$ °C, the ε, γ' and α layers are obtained. At 600 °C, the γ layers are a supplementary source of N atoms which are diffusing inside the workpiece (in the α phase) to harden it.

The ε, γ and γ' layers increase the resistance to wear and the corrosion and decrease the coefficient of friction of the workpiece's surface. The α layer increases the resistance to deep wearing inside the workpiece. In the ion nitriding process, the plasma ions are accelerated in the cathode sheath (the workpiece to be treated) which is then heated by the ion impacts. The key factor in ion nitriding is to control both the production of active species and the temperatures of plasma ions and neutral species.

3.2. Correlations between the N atom density and the thickness of nitrided layers

The neutral radicals are active species which are often present at higher densities than are the ions, as shown in table 1 for a DC N_2 positive column. It can be concluded

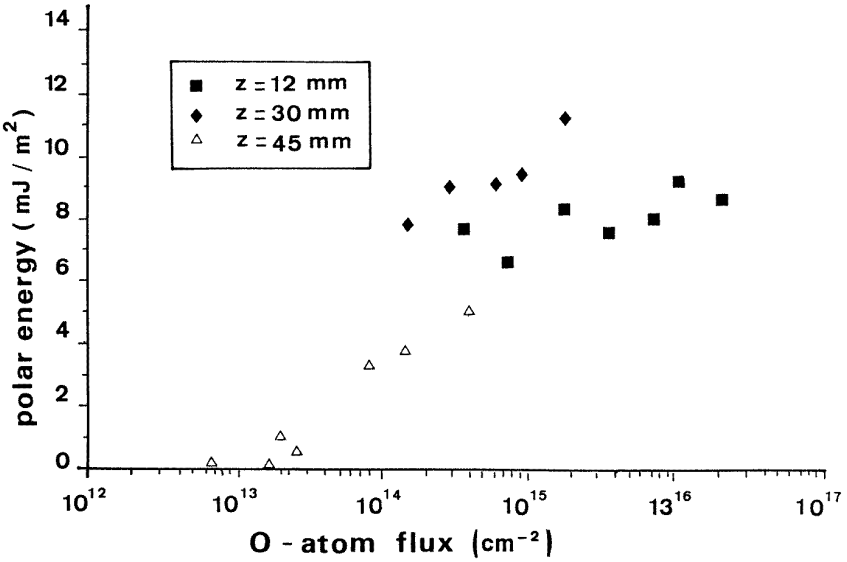

Figure 3. The variation in polar energy of polypropylene with the surface O atom flux (cm^{-2}). z is the position of the substrate in the plasma reactor of figure 1.

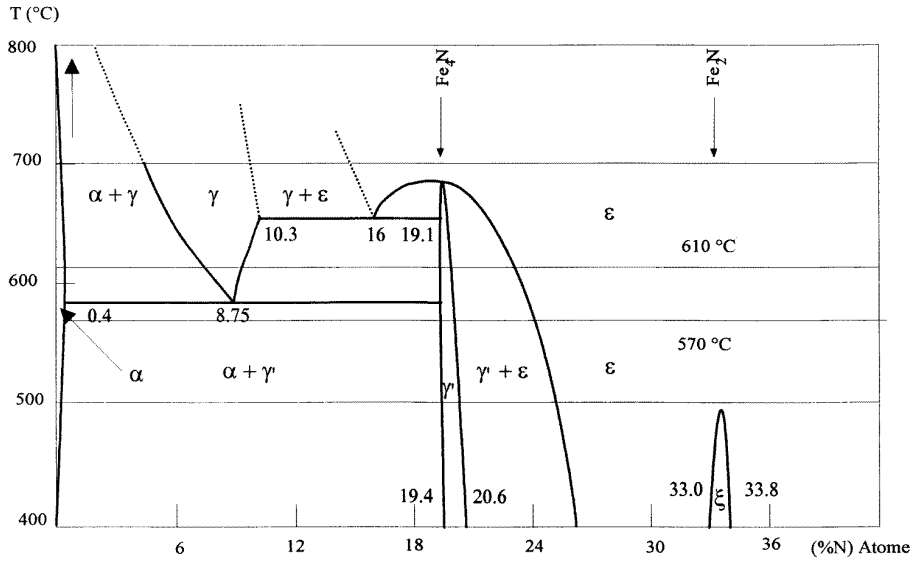

Figure 4. The Fe–N phase diagram.

from the density values in table 1 that the N atoms and N_2 (X,V) vibrational state molecules are the most populous active species in N_2 glow discharges, about 10^4 more prevalent than are N_2^+ ions. Moreover, these excited neutral species are not quickly destroyed on the glass or ceramic tube walls. Also, as for the polymer treatment in post-discharge flowing O_2 (see part 2), post-discharge reactors which separate the plasma, in which the neutral active species are produced, and the workpiece have been set up. Two flowing post-discharge reactors are reproduced in figures 5 and 6. The first one is based on a DC glow discharge (LPGP, Orsay, figure 5) and the second uses a microwave plasma (Ecole des Mines, Nancy, figure 6) [6]. The interest of flowing post-discharge reactors for industrial applications is that workpieces with several surface shapes and features can be treated.

In the post-discharge reactors of figures 5 and 6, the discharges are produced for nitriding processes in N_2 alone or in N_2 mixed with Ar and H_2. The N atoms appear to be efficient nitriding species whose density has been correlated to the quality of nitrided steel coatings [7]. It has been reported [8] that the N atom density can be measured quantitatively by NO titration and by emission spectroscopy in the afterglow region as the result of the following reaction:

$$N + N + M_2 \rightarrow N_2(B, V') + M_2 \qquad (2)$$

$$N_2(B, V') \rightarrow N_2(A, V'') + \text{ first positive system}$$

Table 1. Densities of active species in a DC N_2 positive column (R = 1 cm).

Plasma parameters	
Pressure	0.1–5 Torr
Current density	3.3–50 mA cm^{-2}
Gas temperature	400–700 K
Electric field	10–40 V cm^{-1}
Densities (experimental values)	
N_2 (X)	$n_0 = 3 \times 10^{15}$ to 10^{17} cm^{-3}
e	$n_e = n_i = 10^9$–10^{11} cm^{-3}
N	$n_N = 10^{13}$–10^{15} cm^{-3}
N_2 (A)	$n_A = 10^{11}$–10^{12} cm^{-3}
$N(^2D, ^2P)$	$n_N^* = 10^{10}$–10^{11} cm^{-3}
N_2 (X, V = 10)	$n_{V=10} = 10^{14}$ cm^{-3} (P_{N_2} = 2 Torr, $n_e = 1.7 \times 10^{10}$ cm^{-3}, residence time 10^{-2} s)

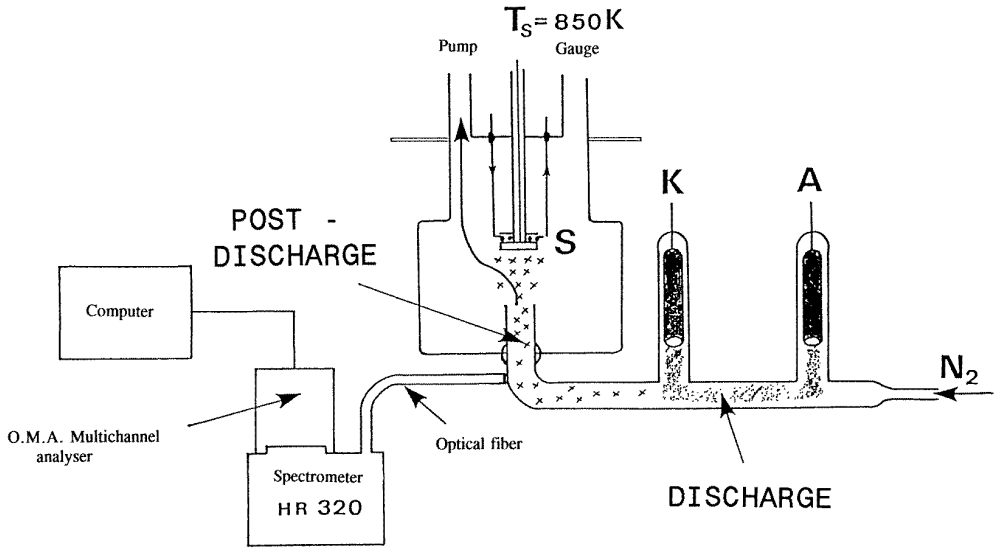

Figure 5. The DC post-discharge reactor for metal-surface nitriding. The discharge tube diameter is 2 cm; the reactor diameter is 15 cm and its length is 20 cm. K, cathode; A, anode; and S, heated substrate.

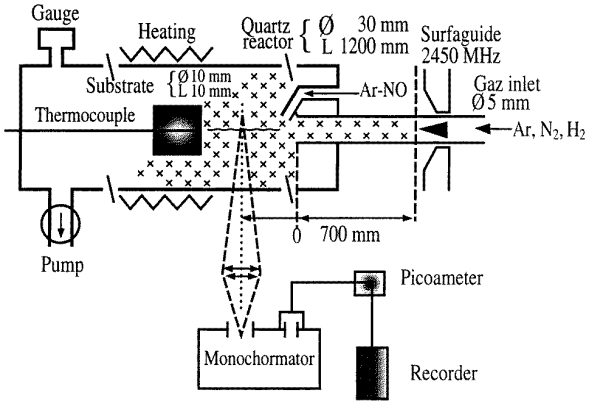

Figure 6. The microwave post-discharge reactor for metal-surface nitriding. The discharge tube diameter is 0.4 cm; the reactor diameter is 3 cm and its length is 100 cm.

where M_2 is a third body (N_2 or Ar). A well-characterized spectrum of the first positive band of N_2 is reproduced in figure 7 for a pure N_2 microwave afterglow [8]. Excitation of N_2 (B,11) is enhanced by reaction (2) and the first positive system emission from this level, mainly the N_2 (B,11)–N_2(A,7), λ = 580.4 nm transition, is considered as a signature of N atoms in the post-discharge region.

Nitriding treatments have been performed with the DC and microwave post-discharge reactors shown in figures 5 and 6. For a N_2 gas pressure of 2.3 Torr and a flow rate Q = 0.3 l min^{-1} similar γ'-Fe_4 N layers of 5–8 μm thickness with α diffusion layers have been obtained in Fe–0.1% C steel substrates heated to 600 °C.

It has been demonstrated [8] that the microwave reactor can work at high gas pressures in Ar–N_2 mixtures, in the range 10–400 Torr with flow rates up to 10 l min^{-1} and at low power (80–200 W). By performing numerous nitriding treatments with the post-discharge reactor of figure 6, the correlation between the γ'-layer thickness and the degree of dissociation of N_2 shown in figure 8 was found. The ε layer appeared when the N:N_2 ratio exceeded 0.01 [6].

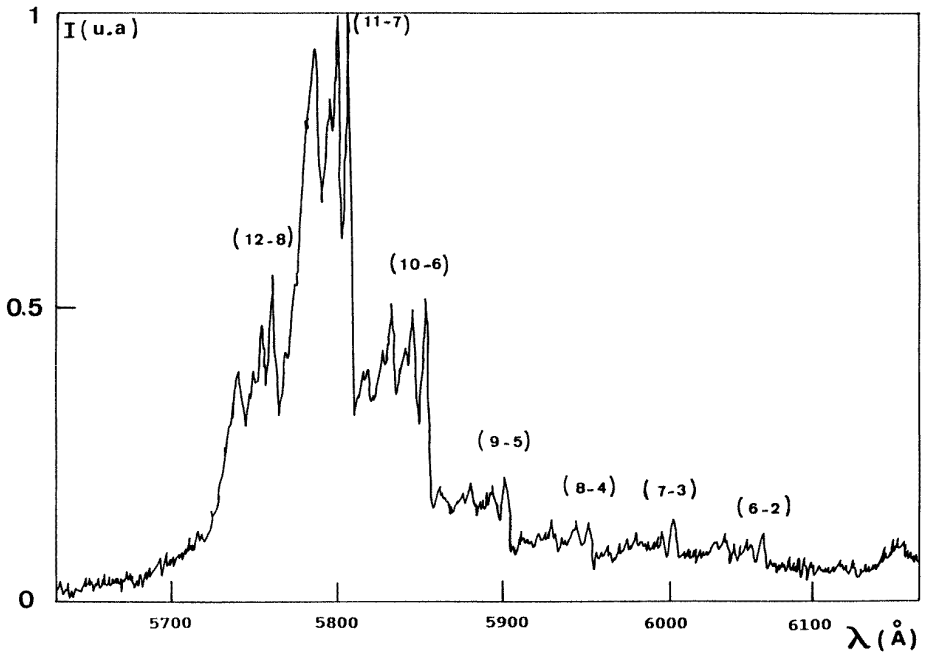

Figure 7. The intensity of the first positive system of N_2 in a flowing post-discharge N_2 plasma.

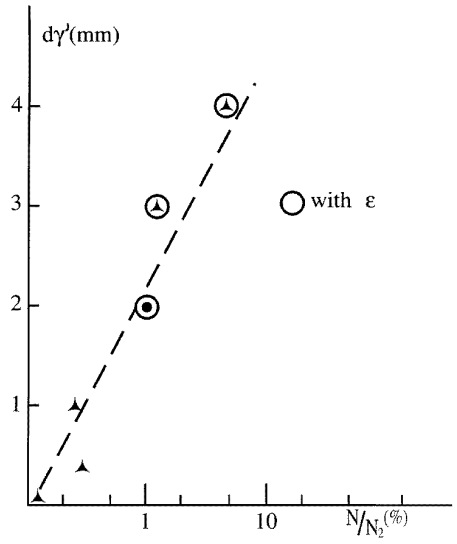

Figure 8. The variations in γ' layer thickness with the percentage degree of dissociation of N_2 in an Ar–N_2 microwave post-discharge plasma.

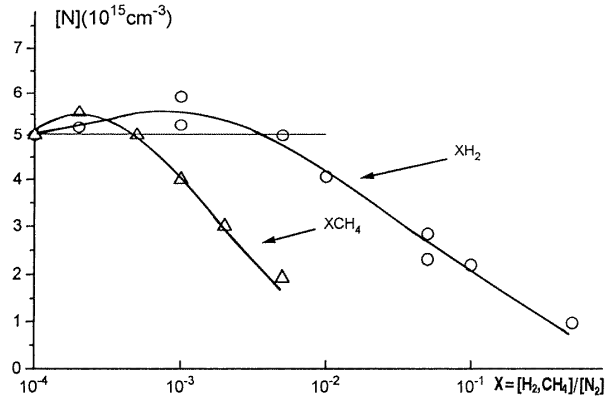

Figure 9. The N atom density versus the H_2:N_2 and CH_4:N_2 density ratios.

3.3. The N atom density and iron coatings with small amounts of CH_4 and H_2 additives in flowing N_2 discharges

In the temperature range for the nitriding process, the steel substrate is very sensitive to oxidation, resulting in part from water and air impurities in the reactor. Thin iron oxide layers (Fe_3O_4) inhibit the nitriding reaction. In order to avoid this problem, H_2 gas was introduced into the N_2 used in the ion nitriding process [5]. It has been found that an addition of only a slight amount of CH_4 [9] or H_2 [10] gas to the N_2 was enough to give impressive results in flowing post-discharge treatments. When a little CH_4 or H_2 gas was introduced into the flowing N_2 HF discharge of figure 6, the N atom density variations reproduced in figure 9 were found (for an Ar–11% N_2–x H_2 or CH_4 post-discharge plasma at $\Delta t = 10^{-2}$ s, 44 Torr and 130 W). First, there is a slow increase in N atom density up to $x = 10^{-3}$ for H_2 and then a sharp decrease for $x > 10^{-2}$. Such a result has also been observed by laser-induced fluorescence (LIF) detection of N atoms in DC and HF N_2–x H_2 post-discharge plasmas, as shown in figure 10 [11]. The increase in N atom density when a little H_2 was introduced into the N_2 positive column at a constant discharge current was interpreted [12] as resulting from an increase in the reduced electric field E/n_0 to maintain the degree of ionization. Indeed, the N_2 (A,a′) and N_2 (X,V) metastable molecules are strongly quenched by H_2. Consequently, there is a decrease in

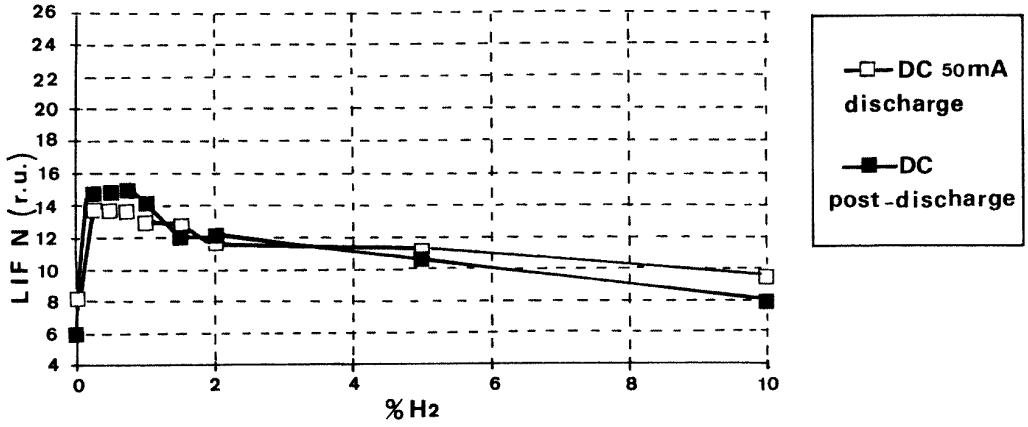

Figure 10. The LIF signal intensity of N atoms versus the percentage of H_2 in a N_2–H_2 DC discharge and under DC and HF post-discharge conditions.

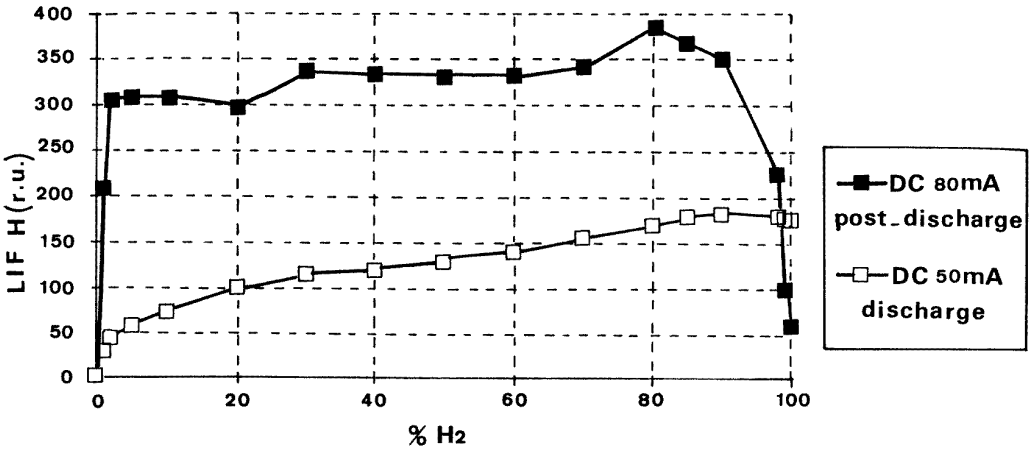

Figure 11. The LIF signal intensity of H atoms versus the percentage of H_2 in a N_2–H_2 DC discharge and under DC and HF post-discharge conditions.

ionization via a two-step route from these metastable levels. Moreover, the following Penning reactions are ineffective:

$$N_2(a') + N_2(a') \rightarrow N_2^+ + e + N_2 \qquad (3)$$

$$N_2(X, V > 30) + N_2(X, V > 30) \rightarrow \begin{cases} N_2^+ + e + N_2 \\ N_4^+ + e. \end{cases}$$

The increase in E/n_0 should then enhance the following electron-induced dissociation of N_2 [13]:

$$e + N_2(X, V) \rightarrow e + N + N. \qquad (4)$$

The determination of the H atom density by LIF is reported in figure 11 for x (H_2) varying in the range 0–100% [11]. A flat maximum in the H atom density, mainly under post-discharge conditions, was found when a little H_2 was introduced into N_2.

Thus, high densities of N and H atoms have been found in N_2 microwave post-discharge plasmas with about 1% H_2. Such results must favour the production of nitrided layers.

Effectively, thick ε nitrided layers without oxides have been obtained with N_2–1%. CH_4 and N_2–1% H_2 gas mixtures, as shown in the micrographs of figures 12 and 13. In figure 12, a pure iron substrate has been treated at 840 K for 3 h in Ar–11% N_2 (figure 12(a)) and Ar–11% N_2–5×10^{-5}% CH_4 (figure 12(b)) gas mixtures in the post-discharge reactor of figure 6. It can be observed in figure 12 that addition of a very small quantity of CH_4 to N_2 greatly increases the thickness of the ε layer to 20–22 μm. The x-ray data in figure 12 show that the Fe_3O_4 peaks are detected for the Ar–11% N_2 case but not for the Ar–11% N_2–5×10^{-5}% CH_4 case. The N and C atom densities in the post-discharge plasma have been determined by NO titration and from chemiluminescent reactions [9]. The following orders of magnitude of atom densities were found: [N] $\approx 10^{15}$ cm^{-3} and [C] $\approx 10^{13}$ cm^{-3}. It can be concluded from the results reproduced in figure 12 that iron oxides are strongly reduced by C and H atoms, allowing an efficient nitriding process.

A pure iron substrate was also treated in the post-discharge reactor of figure 6 for 4 h at 840 K and at a distance $z = 20$ cm in the Ar–11% N_2–x (H_2) post-discharge plasma [10]. Cross sections of iron compounds and diffusion layers are reproduced in figures 13(a)–(c) for

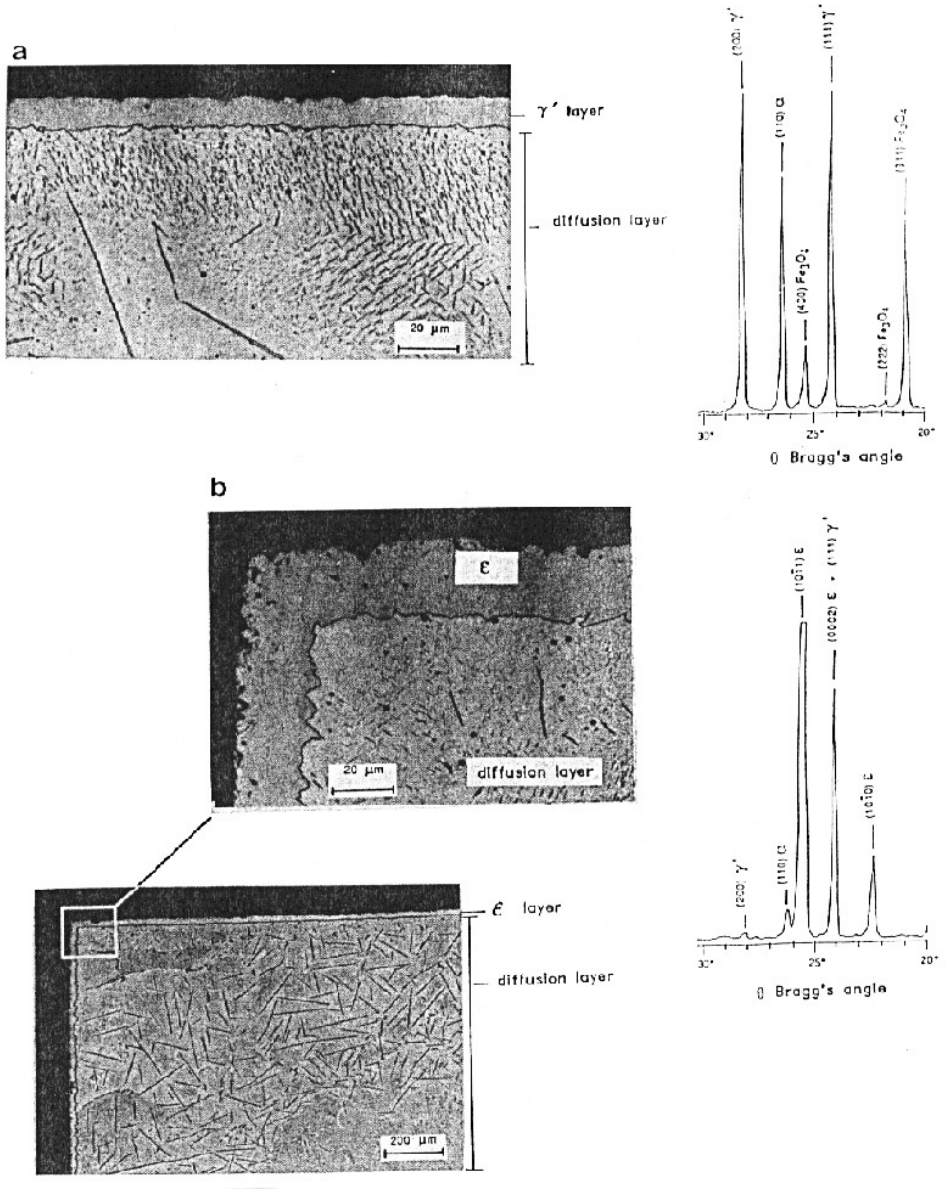

Figure 12. Micrographs of pure iron nitrided by a 3 h treatment in a microwave Ar–N_2–CH_4 post-discharge plasma (the reactor of figure 6, at 130 W, 42 Torr, 3 l min^{-1}, $\Delta t = 10^{-1}$ s): (a) Ar–11% N_2 with [N] = $5(\pm 1) \times 10^{15}$ cm^{-3} and (b) Ar–11% N_2–5×10^{-5} CH_4 with [N] = 4.9×10^{15} cm^{-3} and [C] = 1.6×10^{13} cm^{-3}. X-ray diffraction diagrams are also shown.

$x = 0.5 \times 10^{-3}$ and 5×10^{-2}, respectively. A γ' layer of thickness 3–4 μm was obtained, as shown in figure 13(a), for which a thin outer Fe_4O_3 layer was detected by x-ray analysis. For $x = 5 \times 10^{-3}$ (figure 13(b)) and 5×10^{-2} (figure 13(c)), a thick ε layer (about 10 μm thick) appeared without an oxide layer. Insofar as the ε layer appeared, it seems that oxides are eliminated by H atoms.

4. Atom densities in flowing plasmas with binary gas mixtures of N_2, H_2 and O_2

An increase in N atom density was observed when a little CH_4 or H_2 was introduced into the N_2 flowing discharge (see figures 9 and 10). Also, in a H_2 flowing discharge, the H atom density was increased by adding a little N_2 (see figure 11). With H_2, however, there was a marked difference between the results under discharge and post-discharge conditions. Under discharge conditions, the H atom density remained nearly constant up to 20% N_2 in H_2. At a constant value of the total gas pressure, it can be considered that the dissociation rate of H_2 in the discharge increased in the H_2–< 20% N_2 gas mixture. Under post-discharge conditions, the H atom density greatly increased with a little N_2 in H_2, by more than one order of magnitude, as shown in figure 11. If an increase in electric field in the discharge can be invoked when N_2 is introduced into H_2 [12], the jump in number of H atoms in the flowing post-discharge region must be the result of wall effects. With a little N_2 in H_2, the possible recombination sites of H atoms on the tube walls could be saturated with nitrogen compounds (NH_x).

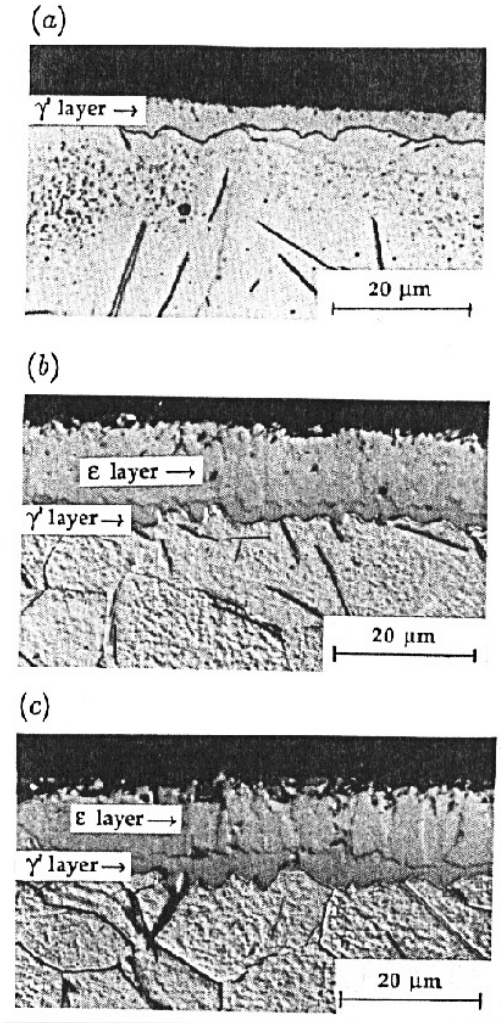

Figure 13. A micrograph of pure iron nitrided by a 4 h treatment in an Ar–N_2–H_2 post-discharge plasma, with discharge parameters as in figure 12: (a) $x = [H_2]/[N_2] = 0$, (b) $x = 5 \times 10^{-3}$ and (c) $x = 5 \times 10^{-2}$.

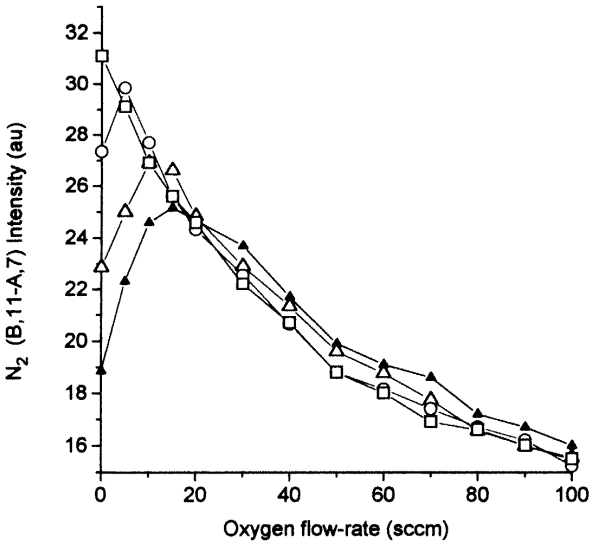

Figure 14. The relative intensity I_{N_2} (B,11–A,7) (proportional to $[N]^2$, see reaction (2)) versus the O_2 flow rate in a N_2–O_2 microwave flowing post-discharge plasma at 4 Torr and 2 l min^{-1} in a borosilicate tube of diameter 1.9 cm. The post-discharge distance was 20 cm. Tube treatment times in the N_2 post-discharge plasma were (□), $t = 0$; (○), $t = 40$ min; (△), $t = 100$ min; and (▲), $t = 460$ min.

An increase by a factor of five in the H atom density when 1% air was introduced into a H_2 microwave discharge (2.45 GHz, 1 Torr, 440 W, tube diameter 16 mm) has recently been observed [14]. From this, a lowering of the probability of destruction of H atoms on the tube wall γ from $\gamma = 2.2 \times 10^{-3}$ in pure H_2 to $\gamma = 2.9 \times 10^{-4}$ in a H_2–1% air gas mixture (at $T = 300$ K) was deduced. The surface chemistry under N_2–H_2 discharge and post-discharge conditions is being investigated [15].

In DC discharges of N_2–O_2 gas mixtures, both an increase in N atom density with a little O_2 in N_2 and an increase in O atom density with a little N_2 in O_2 [16, 17] have also been observed. These experimental results have been interpreted by modelling the plasma volume and surface.

The increase in number of N atoms with a little O_2 ($< 5\%$) in N_2 discharge can be explained in terms of an increase in E/n_0 just like for the N_2–H_2 case [12]. For larger O_2 percentages, the N atom density decreases as a result of destruction processes involving NO and O_2 molecules. Also, the probability of destruction of N atoms on the tube wall γ_N increases with the O_2 content from 10^{-4} in N_2 to 10^{-2} in N_2–($> 20\%$) O_2 [18].

An interesting feature of the increase in N atom density in the flowing N_2–O_2 post-discharge plasma was observed in [17]. The N atom density maximum in a N_2–($< 20\%$) O_2 flowing post-discharge plasma depends on the treatment times of the tube wall, as shown in figure 14. Such results have been interpreted in terms of the removal of absorbed compounds from the surface during the post-discharge treatment. Then the absorption sites of N atoms should be activated, leading to a decrease in N atom density. When a little O_2 is introduced into N_2, the absorption sites might be occupied by oxygen species, producing the increase in N atom densities observed in figure 14.

For O_2 discharges, the probability of destruction of O atoms on the tube wall γ_O has been found to decrease from 4×10^{-3} to 2×10^{-3} at $T = 350$ K when 5% N_2 was introduced into O_2. This decrease in γ_O was related to an increase by about a factor of two in the O atom density [18].

5. Conclusion

In this topical review on plasma technology, two experiments concerning polymer and iron (steel) surface treatments in O_2 and N_2 flowing discharges, respectively, have been reported. Correlations between the production of active plasma species (O in O_2 and N in N_2) and the chemical composition and thickness of the coatings on the treated surfaces have been obtained.

By considering flowing discharge and post-discharge plasmas, the influence of the glass tube walls has been emphasized. With a small addition (in the per cent range) of N_2 or air to H_2, of H_2 or O_2 to N_2 and of N_2 into O_2, a significant increase in density of the atom of the dominant gas has always been observed.

Such effects have been attributed to poisoning of the glass surface by the introduced impurities, strongly reducing the loss of the dominant atoms by heterogeneous reactions on the walls. A study of the surface chemistry involved is in progress. These two examples emphasize the need to control the plasma surface processes by the use of '*in situ*' diagnostics.

References

[1] Peyre J P 1996 *Workshop of Int. Perspectives of Surface Engineering, PSE'96 (Garmisch, Germany)*

[2] Normand F, Granier A, Leprince P, Marec J, Shi M K and Clouet F 1995 *Plasma Chem. Plasma Processing* **15** 173

[3] Granier A, Pasquiers S, Boisse-Laporte C, Darchicourt R, Leprince P and Marec J 1989 *J. Phys. D: Appl. Phys.* **22** 1487

[4] Magne L, Coitout H, Cernogora G and Gousset G 1993 *J. Physique* III **3** 1871

[5] Lebrun J P, Michel H and Gantois M 1972 *Mém. Sci. Rev. Métall.* **69** 727

[6] Ricard A 1995 *Le Vide* **51** 1

[7] Ricard A, Oseguera-Pena J E, Falk L, Michel H and Gantois M 1990 *IEEE Trans. Plasma Sci.* **18** 940

[8] Ricard A, Tetreault J and Hubert J 1991 *J. Phys. B: At. Mol. Opt. Phys.* **24** 1115

[9] Ricard A 1993 *Surf. Coating Technol.* **59** 67–76

[10] Malvos H, Michel H and Ricard A 1994 *J. Phys. D: Appl. Phys.* **27** 1328

[11] Bockel S, Baravian G, Ricard A and Stratil P 1996 *Plasma Sources Sci. Technol.* **5** 567

[12] Garscadden A and Nagpal R 1995 *Plasma Sources Sci. Technol.* **4** 268

[13] Armenise I 1992 *Chem. Phys. Lett.* **200** 597

[14] Tomasini L, Rousseau A, Baravian G, Gousset G and Leprince P 1996 *Appl. Phys. Lett.* **69** 1553–5

[15] Gordiets B F, Pinheiro M J, Ferreira C M, Amorim J and Ricard A 1996 *Escampig XVI (High Tatras, Slovakia)*

[16] Nahorny J, Ferreira C M, Gordiets B, Pagnon G, Touzeau M and Vialle M 1995 *J. Phys. D: Appl. Phys.* **28** 738–47

[17] Supiot P, Dessaux O and Goudmand P 1995 *High Temp. Chem. Processes* **4** 67–73

[18] Gordiets B F, Ferreira C M, Nahorny J, Pagnon D, Touzeau M and Vialle M 1996 *J. Phys. D: Appl. Phys.* **29** 1021–31